

Fermi National Accelerator Laboratory

FERMILAB-Pub-83/42-THY
ITP-SB-83-10
April, 1983

Cancellation of Sudakov Effects in the Drell-Yan Process

ASHOKE SEN

Fermi National Accelerator Laboratory
P.O. Box 500, Batavia, IL 60510

and

GEORGE STERMAN

Institute for Theoretical Physics
State University of New York
Stony Brook, New York 11794

ABSTRACT

We show, by a direct examination of Feynman graphs, that lowest order Sudakov effects factorize from Glauber region gluons in quark-hadron scattering. We then find that the Sudakov double logarithms cancel. The result is consistent with order-by-order factorization in perturbation theory for the Drell-Yan process.



I. INTRODUCTION

Perturbative factorization theorems relate QCD perturbation theory cross sections to the parton model. For short-distance processes such as production of massive μ -pairs and jets in hadron-hadron scattering, they make it possible to calculate scale breaking and, in some cases, relative normalizations. On the other hand, convincing all-order arguments for factorization in hadron-hadron collisions are still lacking. The main problem is to treat the effects of soft gluons. The work of Doria, Frenkel and Taylor¹, and of Bodwin Brodsky and LePage² showed how careful one must be in identifying important regions involving soft gluons. In particular, Bodwin et al. pointed out difficulties in previous factorization arguments³. They discussed "Glauber" exchanges: gluons of predominantly transverse momentum, which attach to spectator quarks of an incoming hadron. Mueller⁴ then observed that the color exchange associated with Glauber gluons induces a further non-cancellation of double logarithmic (Sudakov) bremsstrahlung. He argued that this effect might lead in turn to a buildup of Sudakov suppression for the non-factorizing effects of Glauber exchange gluons. This would restore parton model normalization asymptotically in hadron-hadron processes like Drell-Yan. However, scale breaking in Drell-Yan might be very different from scale breaking in deeply inelastic scattering, at least at present energies². Also, factorization would not hold order-by-order in perturbation theory but would require infinite resummations. This in itself is not such a bad thing, but might make the proof more difficult to extend past the leading logarithm approximation (LLA).

It is our purpose in this paper to show that the treatment of a larger set of graphs than in ref.4 can lead to order-by-order factorization of Sudakov bremsstrahlung from Glauber exchanges. We recover order-by-order "weak" factorization⁵, and argue that Sudakov-like scale breaking need not be present in

complete Drell-Yan and related cross sections. They are, however, present in the restricted set of diagrams analyzed by Mueller⁴ and Date⁶. We should mention that weak factorization in the sense of ref. 5 has been shown to imply "strong" factorization, in which deeply inelastic scattering sets the normalization of the Drell-Yan process.⁷ Also, strong factorization has been verified at two loops for the contributions of gluons whose momenta are not vanishingly small.⁸

We shall work only to the lowest relevant order and in the LLA, but we believe the structure of our calculations indicate that they will apply quite generally. We always work in the Feynman gauge.

Section 2 describes the model in which we work. In section 3 we review the observations of Mueller, and outline our analysis. Sections 4 and 5 describe representative details of the calculation, in the former case for one loop corrections, and in the latter case for two. In section 6 we summarize our results and give a few brief arguments on why we expect them to generalize.

II. THE MODEL

In this section we describe the various approximations and assumptions that we use in our model calculation. We consider the basic graphs shown in Fig. 2.1. Here h is the incoming hadron moving along the $-z$ direction, which couples to the quarks through a vertex W . We assume W falls off rapidly to zero when the transverse momentum flowing through the vertex is large compared to a fixed mass, say the inverse transverse size of the hadron. Otherwise our analysis is independent of the detailed form of the wave function. q is an external quark moving along the $+z$ direction. We work in the centre of mass frame of the external quark and the external hadron, and in the Feynman gauge.

In Feynman gauge, the diagrams shown in Fig. 2.1(a) and 2.1(b) are both of order $\ln^2 s$. The Sudakov double logarithmic contribution comes from the overlap of the regions where the gluons k, k' are either parallel to p or parallel to p' , and the region where k, k' are soft. For definiteness, we consider the overlap region where k is collinear to p and soft (i.e. $k \cdot p \ll k \cdot p' \ll p \cdot p'$).

Although the individual diagrams have double logarithmic contributions from this region, these contributions cancel when we add the two graphs in Fig. 2.1, and we get only a single factorizing log. In this paper we study the effect of adding to the diagram of Fig. 2.1 "exchange" gluons, which are always attached to the spectator quark line at one end and to either the Sudakov gluon or the active quark lines (Fig. 2.2) at the other. If we label the momenta of the exchange gluons by l_i , then these graphs receive leading contribution from three regions in the phase space.

$$\text{Collinear to } p': \quad 1 < l^- < \sqrt{s}; l^+ \sim \frac{1}{\sqrt{s}}; l_{\perp} \sim 1;$$

$$\text{Glauber:} \quad \frac{1}{\sqrt{s}} < l^- \lesssim 1; l^+ \sim \frac{1}{\sqrt{s}}; l_{\perp} \sim 1;$$

$$\text{Infrared:} \quad |l^{\mu}| \lesssim \frac{1}{\sqrt{s}}, \text{ all } \mu,$$

where the scale is set by the cut off on the transverse momentum. In our analysis, we stay away from the IR region, since we expect the contribution from this region to cancel when we sum over real and virtual graphs. We focus our attention on the collinear and the Glauber region.

A consequence of the transverse momentum cut off at W is that both the collinear and Glauber regions for exchange gluons give finite modifications of the $\ln^2 s$ term. Were W a renormalizable vertex, these regions could have led to additional logarithms in their own right,

Below, we refer to the line k^μ as the Sudakov gluon, and to the lines with momentum ℓ_i^μ as the exchange gluons. We assume that the invariant mass of the μ pair, Q , is a finite fraction of \sqrt{s} .

III. REVIEW AND OUTLINE OF CALCULATIONS

Here we review the comments of ref.4 on the interplay of exchange and Sudakov gluons. We then go on to describe our calculations and to give some motivation for them.

We note first that any $q\bar{q}$ scattering amplitude may be written as

$$A_{abcd} = A_1 \delta_{ab} \delta_{cd} + A_8 T_{ab}^i T_{cd}^i, \quad (3.1)$$

with T^i the generators in the fermion representation. In QCD, this decomposes any such amplitude into t-channel singlet and octet representations, as in Fig 3.1. In the discussion below, \underline{A} will represent a generic cut hard process, assumed to be dominated by UV momenta. The simplest example would be the Born term for μ -pair production.

The lowest order Sudakov correction to \underline{A} will be labelled S_{abcd} , and is shown in Fig. 3.2, where k^μ is a Sudakov gluon. Because \underline{A} is UV, the LLA for \underline{S} is simple, and is given by

$$S_{abcd} = A_8 \frac{C_{A8}^2}{8\pi^2} (\ln^2 Q^2) T_{ab}^i T_{cd}^i. \quad (3.2)$$

The octet part of \underline{A} gives rise to non-cancelling Sudakov logs from the correction. These logarithms do not contribute to the cross section at this order, if we average over the colors of the incoming pair;

$$S_{aacc} = \phi(\ln Q^2), \quad (3.3)$$

Thus at lowest order, Sudakov effects cancel. It is only by mixing them with exchange gluons that non-factorizing logs are found.

Still following ref. 4, consider the set of graphs Γ_1 in Fig. 3.3 for quark-hadron scattering. We go to the Glauber region in the momenta k_i^μ . Then a short

calculation shows that in LLA this region gives

$$\Gamma_1 = cA_8 \left(-\frac{C_A}{8\pi^2} g^2 \ln^2 Q \right),$$

where c is a positive constant. It is not difficult to show that as more Sudakov gluons are added to A the result exponentiates, giving

$$cA_8 \exp\left(-\frac{C_A}{8\pi^2} g^2 \ln^2 Q^2\right), \quad (3.4)$$

This is the Sudakov suppression of the Glauber region .

To motivate the calculation described below, we observe that the graphs of Fig. 3.3 do not exhaust the LLA at this order for graphs with a single Sudakov gluon and two exchange gluons attached to spectator quarks. Other graphs, of the form of Fig. 3.4, also contribute in this region. Gluons entering \underline{S} may attach to the bremsstrahlung gluon itself. We call the sum of these graphs Γ_2 . In addition to the Glauber region in the q_1^μ , the collinear region, described in section 2, also contributes in the LLA. (We remind the reader that with limited transverse momenta the collinear region gives a finite, not logarithmic, coefficient to the Sudakov double log.) We should therefore do a calculation which includes collinear, as well as the Glauber regions. This requirement is characteristic of the Feynman gauge.

The result of our calculation is that, in LLA,

$$\Gamma_1 + \Gamma_2 = \frac{1}{3} (S_{aacc})(P_{aa}), \quad (3.5)$$

where P_{ab} is the sum of the graphs shown in Fig. 3.5. The double line represents eikonal propagators of the form⁵

$$\frac{n^\mu}{-n \cdot \ell + i\epsilon}; \quad n^- = -1, \quad n^+ = 1, \quad n^T = 0. \quad (3.6)$$

P_{ab} is the sum of all two loop corrections to the hadron distribution of ref. 5, where the gluons connect the spectator with the eikonal lines. Eq. (3.5) therefore is an example of "weak" factorization, and by eq. (3.3) it has no double logs. It is the factorization of the exchange gluons ℓ_i^μ from the Sudakov gluon k^μ which leads to the form (3.5), in which the Sudakov logs are cancelled.

Now we turn to our method of calculation. First we note that the factorization of eq. (3.5) is easy to derive from the set of graphs in Figs. 3.3 and 3.4 when both ℓ_1^μ and ℓ_2^μ are collinear to p' . This is because collinear exchange gluons carry longitudinal polarization from the bottom of the graph to the top, i.e., their propagators are of the form

$$\frac{g_+^\mu g_-^\nu}{2 \ell_i^2} \approx \frac{n^+}{2 n \cdot \ell_i} \frac{g_+^\mu \ell_i^\nu}{\ell_i^2} \quad (3.7)$$

The approximate equality holds in the collinear region, where

$$n \cdot \ell_i \approx \frac{1}{2} \ell_i^- \quad (3.8)$$

In this case, factorization is just a question of decoupling a set of longitudinally polarized gluons which are inserted into a graph in all possible ways. In an abelian theory, this decoupling is particularly simple, but it occurs as well in the non-abelian case. Here the result is precisely Fig. 3.5 in the collinear region.

This kind of reasoning, of course, cannot be applied when either of the ℓ_i^- vanishes, as in the Glauber region. In this case (3.8), and therefore (3.7), no longer holds, so that the ℓ_i^μ are not longitudinally polarized. To deal with the Glauber region, we use the approach of ref. 5. The definition eq. (3.6) of the eikonal line fixes poles in ℓ_i^- in the upper half plane (UHP) when ℓ_i^μ is defined

to flow out of the eikonal line. Thus, if the k_i^- integration contour is not trapped at $k_i^- = 0$ by a nearby pole in the lower half plane (LHP); it may be deformed into a region where

$$k_i^- \gg k_i^+, k_i^T; \text{Im } k_i^- < 0. \quad (3.9)$$

We denote this as the "complex collinear" region. We shall show below that, after summing over cuts of graphs of the same topology, each k_i^- integration contour may be deformed out of every leading Glauber region, into a complex collinear region like (3.9), always with $\text{Im } k_i^- < 0$. This is true on a graph-by-graph basis for virtual exchange gluons of the graphs of Fig. 3.3⁵. To extend these results to Fig. 3.4, however, requires a sum over cuts. In each complex collinear region, eqs. (3.7) and (3.8) hold, and Ward identities may once again be applied to derive eq. (3.5). The understanding that poles near $k_i^- = 0$ are avoided by deformations into the LHP is summarized in the definition of n^μ and the sign of the $i\epsilon$ in eq. (3.6).

The application of the Ward identities is quite straightforward once the k_i^- integrals are of the desired form (i.e., complex collinear). In the following, we outline a method for combining diagrams to produce expressions in which all leading contributions come from regions where the exchange gluons are complex collinear.

We close this section by pointing out that certain graphs, like Fig. 3.6, which have no double log from the Glauber region, are nevertheless necessary for factorization in the Feynman gauge. This is because they do have double logs when the exchange gluons are collinear. In the Feynman gauge, at least, the Glauber region cannot be considered in isolation.⁹

IV: SINGLE EXCHANGES

In this section, we give a detailed discussion of the single-exchange graphs 4.1(a),(b). The Glauber region for single exchange is associated with an imaginary part, which cancels in the cross section. The manner in which the terms arrange themselves, however, is independent of this cancellation. In fact, the same pattern occurs in the double-exchange graphs like Fig. 4.1(c), which includes a real contribution from a double Glauber region.

As usual, k^μ is Sudakov and ℓ^μ is either Glauber or collinear. As mentioned in sec. 3, in the collinear region, fig. 4.1(a) combines with fig. 4.2 to factor by the Ward identities. Similarly, fig. 4.1(b) should combine with fig. 4.3 to factor. We also need the graphs in fig. 4.4 to get factorization, due to ghost terms in the Feynman gauge Ward identities. (It is easy to check, by examining numerators, that these graphs have Sudakov double logs only when ℓ^μ is collinear, not Glauber.) As we pointed out above, this factorization procedure fails in the Glauber region, where $\ell^- \ll \ell_\perp^2$. To deal with this problem, we examine the positions of poles in the ℓ^- plane.

Since $\ell^+ = o(1/\sqrt{s})$ and $\ell_\perp = o(1)$ in the Glauber region, the pole in ℓ^- from the $1/(\ell^2 + i\epsilon)$ propagator is $o(\sqrt{s})$ from the origin. The same is true for poles of the lower active and spectator quark propagators. Generally, the only poles near the origin in ℓ^- come from the upper active quark and the Sudakov gluon propagators. If all of these poles are in one half plane, we can deform the ℓ^- contour into the opposite half plane all the way to $o(\sqrt{s})$, where one of the other poles may show up. If we look at the relevant poles in ℓ^- from the denominators of $(p-\ell)^\mu$ and $(p-k-\ell)^\mu$ in fig. 4.2(a), for example, they both lie in the UHP. So does the relevant ℓ^- pole from $(p-k-\ell)^\mu$ in fig. 4.2(b). Hence, in these graphs the ℓ^- contour may be deformed into the LHP, all the way to $o(\sqrt{s})$ in the complex collinear region.

In Fig. 4.1(a), however, the ℓ^- pole from the denominator of the line $(k+\ell)^\mu$ lies in the lower half plane at a distance $o(k_1^2/k^+)$ from the origin. As a result, if we want to deform the ℓ^- contour into the lower half plane, so as to make it coincide with the ℓ^- contours in Figs. 4.2(a) and (b), we must pass through the pole from the denominator $(k+\ell)^\mu$. We then have to include an extra contribution from the residue at this pole. A similar problem occurs when we try to combine the contribution from Fig. 4.1(b), with the contribution from the graph of Fig. 4.3(a), since the ℓ^- pole from the denominator of the line $(p+\ell)^\mu$ in Fig. 4.3(a) lies in the upper half plane, while the ℓ^- pole from the denominator of $(k-\ell)^\mu$ in Fig. 4.1(b) lies in the lower half plane. We shall show that when we add all the graphs, these extra contributions cancel and we are left with contributions that can be factored by the use of Ward identities.

We use a diagrammatic method for doing our calculation. First we do the ℓ_0 integral by closing its contour in one half plane or the other and picking up various poles coming from the Feynman denominators. Leading contributions will be associated with poles in denominators left in the resulting expression. It is now important to note that, after we close on the ℓ_0 contour, the effective prescription for some other Feynman denominators may change. To see how this may happen, let us consider a simple double integral

$$\int \frac{dx}{x-i\epsilon_1+y/2} \frac{dy}{x+y+i\epsilon_2} \frac{1}{x-a+i\epsilon_3} \quad , \quad (4.1)$$

and suppose we choose to close the x integration contour on the lower half plane. The two poles that lie in the lower half plane are

$$x = a-i\epsilon_3, \quad -y-i\epsilon_2. \quad (4.2)$$

Then (4.1) may be written as

$$-(2\pi i) \left[\int \frac{1}{a + \frac{y}{2} - i(\epsilon_3 + \epsilon_1)} \frac{dy}{a + y + i(\epsilon_2 - \epsilon_3)} + \int \frac{1}{-y/2 - i\epsilon_1 - i\epsilon_2} \frac{1}{-y - a + i(\epsilon_3 - \epsilon_2)} \right]. \quad (4.3)$$

If we take $\epsilon_3 > \epsilon_2$, then the effective $i\epsilon$ prescription for the $(x+y+i\epsilon_2)^{-1}$ denominator changes sign in the first term of (4.3). The $i\epsilon$ prescription for the term $x-i\epsilon_1+y/2$ does not change sign. The final result, however, does not depend on whether ϵ_2 is greater than or smaller than ϵ_3 , when we add the two terms in (4.3). This is a general feature. We can assume any relative orders of magnitude of the $i\epsilon$'s in the Feynman denominators in our calculation, instead of taking them to be equal, provided we consistently follow the same convention within each graph. This is best seen by going to the Feynman parameter representation of the integral, where the integrand looks like

$$\left[\sum_{i=1}^n \alpha_i (\ell_i^2 - m_i^2 + i\epsilon_i) \right]^{-1}. \quad (4.4)$$

Thus, so long as the ϵ_i 's are positive, $\sum_{i=1}^n \alpha_i \epsilon_i$ is positive, and we get the same final answer, independent of the relative magnitudes of the ϵ_i 's that we choose.

Let us now examine a Feynman integral,

$$\int \frac{dk^0}{\{(k^0)^2 - \vec{k}^2 - \mu^2 + i\epsilon_1\} \{(p^0 - k^0)^2 - (\vec{p} - \vec{k})^2 - \mu^2 + i\epsilon_2\}}. \quad (4.5)$$

We assume that $\epsilon_1 \gg \epsilon_2$, and close the k^0 contour in the lower half plane. We consider the contribution from the pole at $k^0 = \sqrt{\vec{k}^2 + \mu^2} - i\epsilon_1$. The contribution

from the other denominators may be written as

$$\frac{1}{(k^0 + \sqrt{k^2 + \mu^2 - i\epsilon_1})(p^0 - k^0 - \sqrt{(\vec{p} - \vec{k})^2 + \mu^2 + i\epsilon_2})} \frac{1}{(p^0 - k^0 + \sqrt{(\vec{p} - \vec{k})^2 + \mu^2 - i\epsilon_2})} \cdot \quad (4.6)$$

The result of closing the k^0 contour on the pole at $k^0 = \sqrt{k^2 + \mu^2 - i\epsilon_1}$ may then be written as

$$\begin{aligned} & (-2\pi i) \delta(k^2 - \mu^2) \theta(k_0) \{k^0 + \sqrt{k^2 + \mu^2 - i\epsilon_1}\}^{-1} \\ & \times \{p^0 - k^0 - \sqrt{(\vec{p} - \vec{k})^2 + \mu^2 + i\epsilon_1}\}^{-1} \{p^0 - k^0 + \sqrt{(\vec{p} - \vec{k})^2 + \mu^2 + i\epsilon_1}\}^{-1} \end{aligned} \quad (4.7)$$

The correctness of (4.7) may be verified by replacing k^0 by $\sqrt{k^2 + \mu^2 - i\epsilon_1}$ in (4.6) and using the fact that $\epsilon_1 \gg \epsilon_2$.

We generalize this procedure by strongly ordering all the ϵ 's:

$$\epsilon_a \gg \epsilon_b \gg \epsilon_c \dots,$$

and linearizing denominators in the ℓ_i^0 , as in Eq. (4.6). Then the following rule allows us to keep track of the $i\epsilon$'s at each stage in the integrations.

If $\epsilon_i \gg \epsilon_j$ for $i > j$, and $\eta_i = \pm 1$,

$$\begin{aligned} & \frac{1}{2\pi i} \int_{-\infty}^{\infty} d\ell_0 \prod_{i=1}^n [\ell_0 - a_i + i\epsilon_i \eta_i]^{-1} \\ & = \sum_{i=1}^n \eta_i \prod_{j=1}^{i-1} [a_i - a_j + i\epsilon_j \eta_j]^{-1} \prod_{k=i+1}^n [a_i - a_k - i\epsilon_i \eta_i]^{-1}. \end{aligned}$$

That is, when pole i is taken, ϵ_i (including sign) simply replaces all ϵ_k with $k < i$ on all other lines which carry ℓ_0 . Lines with $\epsilon_j > \epsilon_i$ retain their $i\epsilon$ prescription unchanged. In this way we avoid θ -functions involving differences of the ϵ 's, all of which must cancel in the final result.

When we represent the result of an energy integral in terms of diagrams, we shall put a slash (/) on a line whose $i\epsilon$ prescription has changed sign. If it changes sign in only one of the two terms into which a Feynman denominator breaks up (as in the example above) we shall put an arrow, together with the slash, in the direction of the energy flow on the term whose $i\epsilon$ prescription changes sign.

We shall make the following approximation in our calculation. We are interested in the region of integration where the Sudakov gluon k^μ and the quark lines $q^\mu, (p'-q)^\mu, p^\mu$ carry large energy from the left to the right in the diagrams. Other regions of integration cannot contribute to the LLA because of the transverse momentum cutoff at the "wave function". Hence, when we close the ℓ_0 contour, we shall ignore poles which require the energy of these lines to flow in the opposite direction. We then express the ℓ_0 integral as a sum of several diagrams, in each of which an allowed pole has been taken. In these diagrams, the Sudakov gluon line connecting the exchange gluon and the fermion line generally does not have the correct $i\epsilon$ prescription to allow the exchange gluons to factor. To deal with this problem, we express its denominator as a sum of two terms. One term has the $i\epsilon$ prescription reversed, and the other is a δ function, using

$$(x - i\epsilon)^{-1} = (x + i\epsilon)^{-1} + 2\pi i\delta(x). \quad (4.8)$$

Using all the prescriptions mentioned so far, the contribution from Fig. 4.1(a) may be evaluated as in Fig. 4.6. The precise Feynman rules for the various

special propagators are shown in Fig. 4.5. They are valid when the line lies to the left of the cut. When the line lies to the right of the cut we must complex conjugate the expression given in Fig. 4.5. Also, a circled propagator, as in Fig. 4.6, tells us that the line cannot be on-shell. The numbering of the different lines in Fig. 4.6(a) is according to the order of increasing ϵ , i.e. we have $\epsilon_5 \gg \epsilon_4 \gg \epsilon_3 \gg \epsilon_2 \gg \epsilon_1$.

Of the diagrams in Fig. 4.6, the contribution from Fig. 4.6(c) does not have the problem of having wrong $i\epsilon$ sign for line 4 (where by wrong we mean opposite to what we need for factorization). This is because in Fig. 4.6(c) this line is kinematically prevented from being on-shell and hence combines with other similar graphs, shown in Fig. 4.7, to factor.

The contribution from Fig. 4.6(d) is suppressed. This can be seen in the following way. After we substitute the δ function for the Feynman propagator for line 5, we may express the integral in terms of ℓ^\pm variables (see Fig. 4.1) instead of ℓ^0 and ℓ^3 variables. The δ function then constrains ℓ^- to be equal to $-(\underline{p}_1 - \underline{k}_1 - \underline{\ell}_1)^2 / (p^+ - k^+) - \underline{k}_1^2/k^+ + p_2^-$, which is independent of ℓ^+ , so long as $|\ell^+| \ll |p^+|$. The contribution from line 4 is also independent of ℓ^+ if $|k^+| \gg |\ell^+|$. The ℓ^+ pole from the denominators of the lines 1, 2 and 3, all lie on the same side of the real axis. Thus the ℓ^+ contour may be deformed away from the origin up to a distance of order k^+ . The contribution to the graph from this region is not a leading log. A detailed calculation is given in the appendix.

We are then left with the contribution from Fig. 4.6(b). This has the wrong $i\epsilon$ sign for the line 4, so we reduce the Feynman propagator for line 4 using the identity eq. (4.8). Fig. 4.6(b) may then be expressed as the sum of the graphs shown in Fig. 4.8. Fig. 4.8(a) has the correct $i\epsilon$ prescription and combines with other graphs (similar to the ones shown in Fig. 4.7,

except that the bottom quark line is on-shell, rather than the gluon line carrying momentum ℓ) and factor. We are then left with the contribution from Fig. 4.8(b) as the only term from Fig. 4.1(a) with a non complex-collinear leading part.

We can now turn to the graph of Fig. 4.1(b) and do the ℓ_0 integral to express it as a sum of the graphs shown in Fig. 4.9. Fig. 4.9(b) may be factorized by combining it with other graphs, since the right part of the Sudakov gluon line is prevented from being on-shell, so that the sign of the $i\epsilon$ in the denominator is irrelevant. Fig. 4.9(a) may be expressed as a sum of the graphs shown in Fig. 4.10. Of these, Fig. 4.10(b) has the correct $i\epsilon$ prescription for the Sudakov gluon to combine with the other graphs and factor. Fig. 4.10(a) is identical to Fig. 4.8(b), except for a minus sign, and they cancel. This minus sign comes from the changes in sign of the propagator of the exchange gluon line and of the vertices at which it attaches to the Sudakov gluon and to the spectator quark line. Since the exchange gluon is prevented from being on-shell by kinematics, the relative sign of $i\epsilon$ in the exchange gluon denominators in Figs. 4.10(a),(b) does not affect the cancellation. This eliminates all terms from Figs. 4.1(a),(b) with non complex-collinear leading parts.

This type of cancellation, which is crucial for factorization, seems to be quite general. In the next section, we show that this cancellation occurs when we sum over all graphs with one Sudakov gluon and two exchange gluons.

V. DOUBLE EXCHANGES

In this section we shall take into account the effects of two loop corrections to the basic graphs shown in Fig. 2.1. The relevant graphs may be divided into three classes: (1) Both the exchange gluons attached to the active quark (2) One of the exchange gluons attached to the active quark, the other one attached to the Sudakov gluon and (3) both the exchange gluons attached to the Sudakov gluon. Of these, in the graphs of class 1, the gluon momenta may always be deformed to the complex collinear region.⁵ Graphs of type 2 may be analyzed in the same way as we analyzed the one loop graphs in Sec. 4. Hence in this section we shall concentrate on the graphs of type 3, examples of which are shown in Fig. 5.1,

To keep our discussion brief, we shall consider only the diagrams shown in Fig. 5.2, and will show how we can bring them into a form where the momenta can readily be deformed into the complex collinear region, and factorization may be achieved,

As in Sec. 4 we number the lines in the order of increasing $i\epsilon$, $\epsilon_1 \ll \epsilon_2 \ll \epsilon_3 \ll \epsilon_4 \ll \epsilon_5$. We first integrate over the k_1^0 and the k_2^0 momenta, using this ordering of the ϵ 's. We then analyze each term obtained by the integration, and bring it into a form where the momentum contours may be deformed into the complex collinear region. In doing this, we have to change the $i\epsilon$ prescription of some of the lines in the same way we did in Sec. 4. The following relations are useful, along with eq. (4.8),

$$\frac{i}{x+i\epsilon} \frac{i}{y+i\epsilon} = \frac{i}{x-i\epsilon} \frac{i}{y-i\epsilon} + \frac{i}{x-i\epsilon} 2\pi\delta(y) + 2\pi\delta(x) \frac{i}{y+i\epsilon} , \quad (5.1)$$

$$\frac{(-i)}{x-i\epsilon} \frac{i}{y+i\epsilon} = \frac{(-i)}{x+i\epsilon} \frac{i}{y-i\epsilon} + 2\pi\delta(y) \frac{(-i)}{x-i\epsilon} + 2\pi\delta(x) \frac{i}{y-i\epsilon} . \quad (5.2)$$

We start with Fig. 5.2(A), which we call diagram A. After we do the ℓ_2^0 integral, we get terms A1, A2, A3 and A4 shown in Fig. 5.3. In each of these, we do the ℓ_1^0 integral, and get the terms A1a, A1b, ... A4a, also shown in Fig. 5.3. Of these, the terms A2b and A3b are not leading logarithm, since the ℓ_1^+ contour is not pinched and hence may be deformed away to $o(\sqrt{k^+})$. Similarly, A4a is suppressed, since the ℓ_2^+ contour may be deformed to $o(\sqrt{k^+})$. In addition, A3a does not contribute to leading log, because the arrangement of poles in this case prevents the ℓ_i^+ from being either Glauber or collinear to the bottom spectator.

Ignoring these terms, we use eqs. (4.8), (5.1) and (5.2) to generate a set of terms with the correct $i\epsilon$ signs on the Sudakov lines to give factorization. These are shown in Fig. 5.4, while the remaining, non-factorizing terms are shown in Fig. 5.5. Of these terms, (1) and (2) come from A1a in Fig. 5.3, terms (3) and (4) come from A1b, term (5) comes from A1c, and terms (6) and (7) come from A2a.

We may repeat the same analysis for Figs. 5.2(B) and (C). Their left-over terms, analogous to Fig. 5.5 are shown in Figs. 5.6 and 5.7, respectively.

We now note the following cancellations, which eliminate most of the left-over terms in Figs. 5.5, 5.6 and 5.7.

$$\begin{aligned}
 (2) + (12) &= 0 & (7) + (11) &= 0 \\
 (3) + (14) &= 0 & (8) + (13) &= 0 \\
 (4) + (9) &= 0 & (10) + (17) &= 0 \\
 (5) + (16) &= 0
 \end{aligned}$$

In writing down the above equation, we have used the fact that the vertices and the Feynman propagator acquire a relative minus sign when they cross the cut, as does the $i\epsilon$ in the Feynman denominator. For example, the slash on the

right exchange gluon in (12) is important. Since this gluon is to the left of the cut in (2) and to the right of the cut in (12), the net effect is that the $i\epsilon$ prescription is the same in (2) and (12) for the pole where the energy of this gluon flows up. There is a relative minus sign in the $i\epsilon$'s in the pole where the energy flows down, but in this region the line is kinematically prevented from being on-shell.

Thus, we are left with the terms (1), (6), (15) and (18). Each of these terms has an intermediate state with three on-shell lines. These terms cancel with terms coming from cut diagrams with three real lines (e.g. the one shown in Fig. 5.8), when we go through the same analysis for them. Through our sample calculation, we have shown how to bring the graphs into a form suitable for factorization. All other terms are treated in an exactly similar way.

VI. DISCUSSION

We have shown by direct calculation that, to lowest relevant order and leading logarithm, Glauber exchanges are consistent with weak factorization even in the presence of a Sudakov gluon. We believe the pattern of the calculation is sufficiently organized to conjecture that this result is quite general.

The mechanism of factorization may be summarized as follows. Momentum space contours for exchange gluons are deformed from the Glauber into the complex collinear region, leaving behind various pole contributions, all of which are due to the presence of the Sudakov gluon. Then:

(1) The left-over poles cancel in the sum over graphs with the same topology but different cuts, and

(2) The complex collinear gluons factor by the use of Ward identities.

Aside from the simplicity of this pattern at lowest order, one may also argue more generally, if heuristically, based on the work of Ellis, De Tar, and Landshoff, and Cardy and Winbow.¹⁰ In our calculation, a Sudakov gluon acts like a spectator; it is relatively energetic over its whole energy range, and nearly parallel to the top incoming hadron. On the other hand, a Glauber region gluon may be compared to a pomeron; it carries spacelike momentum and thus cannot go on-shell. The case of pomerons interacting with spectators has been treated by Ellis et al.¹⁰ They use a rather different language than we do, but their argument still comes down to the analytic properties of Feynman integrals. They conclude that after a sum over cuts of graphs of the same topology, it is always possible to deform from a region where small momentum flows through a pomeron into a region where large, (nearly lightlike) momentum flows through it. This result that contour deformation is possible is theory-independent. It is true in renormalizable as well as super-renormalizable theories, and in non-abelian as well as abelian gauge theories.

The ability to deform contours after summing over cuts implies the cancellation of left-over poles mentioned in (1) above. Ellis et al. do not sum over cuts of different topology as we do to get (2), because complex collinear contributions are suppressed by power counting in the super-renormalizable case which they assume.

We have carried out our analysis using covariant perturbation theory. One might wonder what happens in time-ordered perturbation theory. In particular, we expect final state interactions to cancel in time ordered perturbation theory, leaving over various initial state interactions which are naturally associated with Glauber exchanges before the hard interaction.² Our calculation implies simply that initial state as well as final state interactions can combine in a non-trivial way across the cuts. This does not contradict the possibility of independent initial state factorization on each side of the cut,² but suggests that identities exist which allow alternative organization of the relevant terms.

We can give a suggestive example of this mechanism by studying Figs. 4.1(a) and (b). In Fig. 4.1(a) when ℓ^μ is a Glauber gluon it may be in either the initial or final state. In Fig. 4.1(b), however, ℓ^μ gives only a final state interaction when k^μ is Sudakov. This is because any state involving the line $(q-k)^\mu$ is off-shell in that region. One finds then that the final state contributions cancel, leaving the initial state contribution from Fig. 4.1(a). This term is exactly the imaginary part of the deformable, complex collinear, term Fig. 4.1(b), which combines with Fig. 4.3 to factor. In a sense, then, it is precisely ~~the~~ initial state term from Fig. 4.1(a) which combines with Fig. 4.3 to give the fully factored result.

Acknowledgements

We wish to thank Goeff Bodwin, Stan Brodsky, John Collins, Peter LePage, Al Mueller and Dave Soper for useful conversations, which led to this work. This work was supported in part by the Department of Energy and by the National Science Foundation.

APPENDIX

In this appendix we shall show that the contribution from Fig.4.6(d) is suppressed. To do this, let us label the momenta in the graph as in Fig.A.1. Then the contribution from the line carrying momentum $p-k-l$ is given by

$$2\pi \delta[(p-k-l)^2 - m^2] \approx 2\pi (p^+ - k^+)^{-1} \delta(p^- - k^- - l^- - \frac{(p-k-l)_\perp^2 + m^2}{p^+ - k^+}) \quad (\text{A.1})$$

in the region $|\ell^+| \ll |k^+|, |p^+|$. The denominator of the line $(k+l)^\mu$ is independent of ℓ^+ in the region. Thus the only ℓ^+ dependent denominators come from the lines carrying momentum $\ell^\mu, (p'-q-\ell)^\mu$ and $(q+l)^\mu$. Taking into account the change in sign of the $i\epsilon$ in the denominators of the lines ℓ^μ and $(p'-q-\ell)^\mu$ we may write the total contribution from these denominators as

$$\begin{aligned} & (\ell^+ \ell^- - \vec{\ell}_\perp^2 - \mu^2 + i\epsilon \ell^-)^{-1} \{ (p'^- - q^- - \ell^-) (p'^+ - q^+ - \ell^+) - \frac{(p'-q-\ell)_\perp^2 + m^2}{p^+ - k^+} \} \\ & - i\epsilon (p'^- - q^- - \ell^-) \}^{-1} \{ (q^+ + \ell^+) (q^- + \ell^-) - (\vec{q}_\perp + \vec{\ell}_\perp)^2 - m^2 + i\epsilon \}^{-1}. \end{aligned} \quad (\text{A.2})$$

Thus the pole in the ℓ^+ plane always lies in the lower half plane and we may close the ℓ^+ contour in the upper half plane. The numerator is effectively ℓ^+ -independent, and the powers of ℓ^+ in the denominator would be sufficient to make the integral vanish if the deformation were extended to infinity. The approximation we have made, however, is valid only in the region $|\ell^+| \ll |p^+|, |k^+|$. Thus we cannot really close the contour at infinity, but can at least deform the ℓ^+ contour away from the origin to a distance $o(k^+)$. In this region, the contribution from the graph of Fig. A.1 is no longer leading logarithm, as may easily be seen by a direct examination of the integrals.

REFERENCES

- ¹R. Doria, J. Frenkel and J.C. Taylor, Nucl. Phys. B168 (1980) 93.
C. Di'Lieto, S. Gendron, I.G. Halliday and C.T. Sachrajda, Nucl. Phys. B183 (1981) 223.
- ²G.T. Bodwin, S.J. Brodsky and G.P. Lepage, Phys. Rev. Lett., 47 (1981) 1799.
- ³D. Amati, R. Petronzio, and G. Veneziano, Nucl. Phys. B140 (1978) 54, B146 (1978) 29. S. Libby and G. Sterman, Phys. Rev. D18 (1978) 3252; ibid 4737.
A.H. Mueller, Phys. Rev. D18 (1978) 3705.
R.K. Ellis, H. Georgi, M. Machacek, H.D. Politzer and G.G. Ross, Nucl. Phys. B152 (1979) 285.
A.V. Efremov and A.V. Radyushkin, Theor. and Math. Phys. 44 (1981) 664; ibid 774.
- ⁴A.H. Mueller, Phys. Lett. 108B (1982) 355.
- ⁵J.C. Collins, D.E. Soper and G. Sterman, Phys. Lett. 109B (1982) 388, and Stony Brook Report ITP-SB-82-46 (1982).
- ⁶G. Daté, Stony Brook Report ITP-SB-82-47 (1982), to be published in Phys.Rev.
- ⁷J.C. Collins, D.E. Soper and G. Sterman, Oregon preprint OITS 209 (1983) (to be published in Phys. Lett.)
- ⁸W.W. Lindsay, D.A. Ross and C.T. Sachrajda, Phys. Letts. 117B (1982) 165, Nucl. Phys. B (to be published), and Southampton preprint SHEP 82/83-4 (1983).
- ⁹C.A. Nelson, SUNY Binghamton Report SUNY BING 11/25/82 (1982).
- ¹⁰C.E. DeTar, S. D. Ellis and P.V. Lanshoff, Nucl. Phys. B87 (1975) 176.
J.L. Cardy and G.A. Winbow, Phys. Lett. 52B (1974) 95.

FIGURE CAPTIONS

- Fig. 2.1 Lowest order graph with Sudakov double logarithms.
- Fig. 2.2 Examples of graphs found by adding exchange gluons to Fig. 2.1.
- Fig. 3.1 Color decomposition of quark-antiquark scattering.
- Fig. 3.2 Definition of \underline{S} .
- Fig. 3.3 Graphs included in Γ_1 .
- Fig. 3.4 Graphs included in Γ_2 .
- Fig. 3.5 Definition of P_{ab} in eq. (3.5).
- Fig. 3.6 Graph with double log but no Glauber region in the Feynman gauge.
- Fig. 4.1 Single exchange graphs and a related double exchange graph.
- Fig. 4.2 Single exchange graphs related by Ward identity to Fig. 4.1(a).
- Fig. 4.3 Graphs related by Ward identity to Fig. 4.1(b).
- Fig. 4.4 Graphs required for factorization in the Feynman gauge.
- Fig. 4.5 Definition of graphical notation.
- Fig. 4.6 Result of energy integral on Fig. 4.1(a) with indicated choice of ε 's.
- Fig. 4.7 Set of factoring graphs.
- Fig. 4.8 Use of eq. (4.8) on Fig. 4.6(b).
- Fig. 4.9 Result of energy integral on Fig. 4.1(b).
- Fig. 4.10 Use of eq. (4.8) on Fig. 4.9(a).
- Fig. 5.1 Graphs of type 3.
- Fig. 5.2 Cuts of Fig. 5.1(a) discussed in text.
- Fig. 5.3 Result of energy integrals on diagram A.
- Fig. 5.4 Diagrams in which ℓ^- contours can be deformed into the LHP.
- Fig. 5.5 Diagrams left over after isolating Fig. 5.4 from Fig. 5.3 by using eqs. (4.8), (5.1) and (5.2).

Fig. 5.6 Diagrams left over from Fig. 5.2(B).

Fig. 5.7 Diagrams left over from Fig. 5.2(C).

Fig. 5.8 Graph with cut exchange gluon.

Fig. A.1 Suppressed diagram discussed in text.

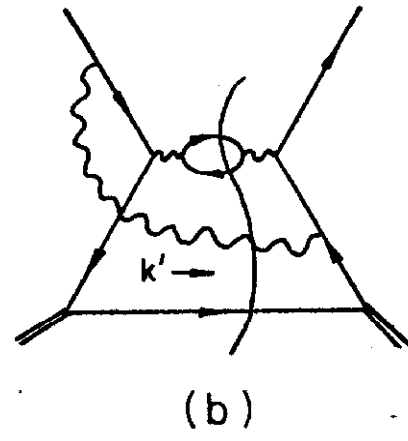
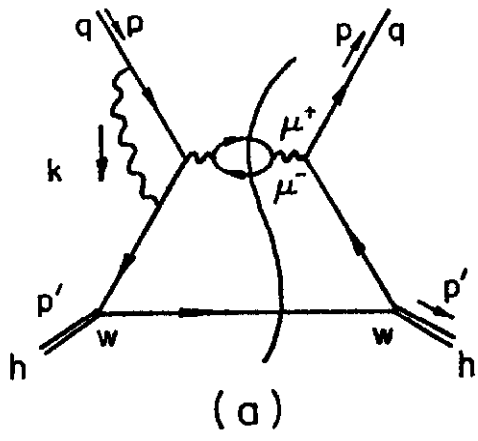


FIG. 2.1

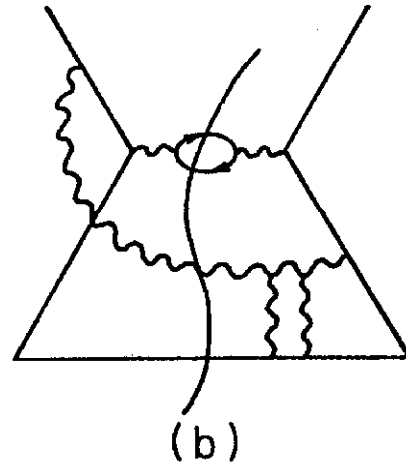
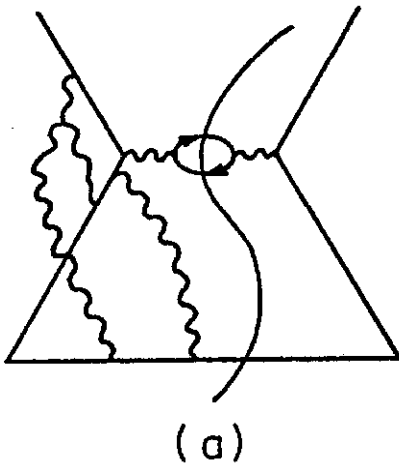


FIG. 2.2

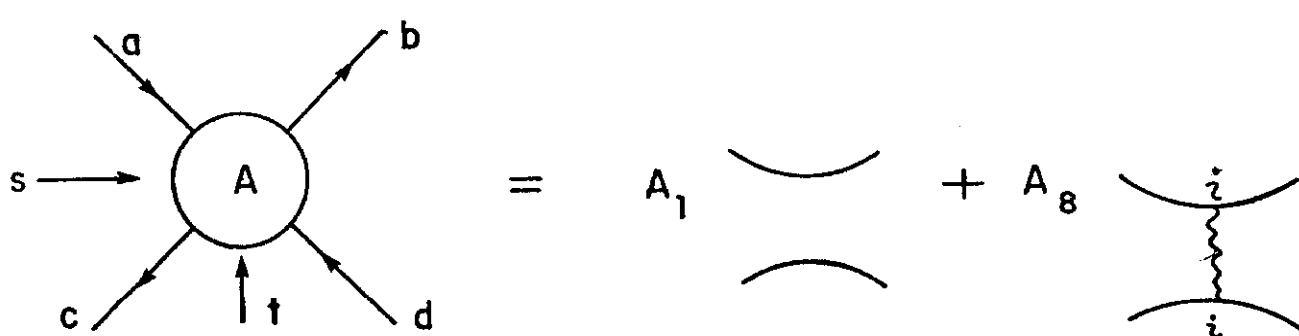
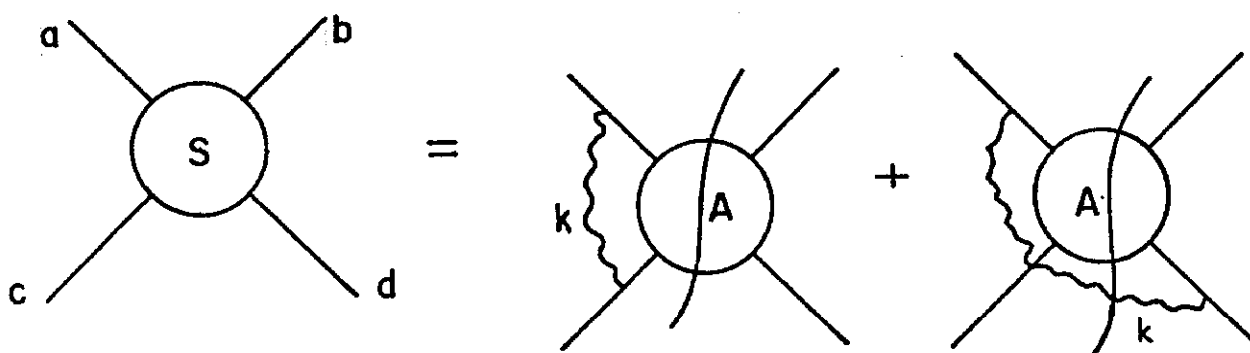


FIG. 3.1



+ MIRRORS

FIG. 3.2

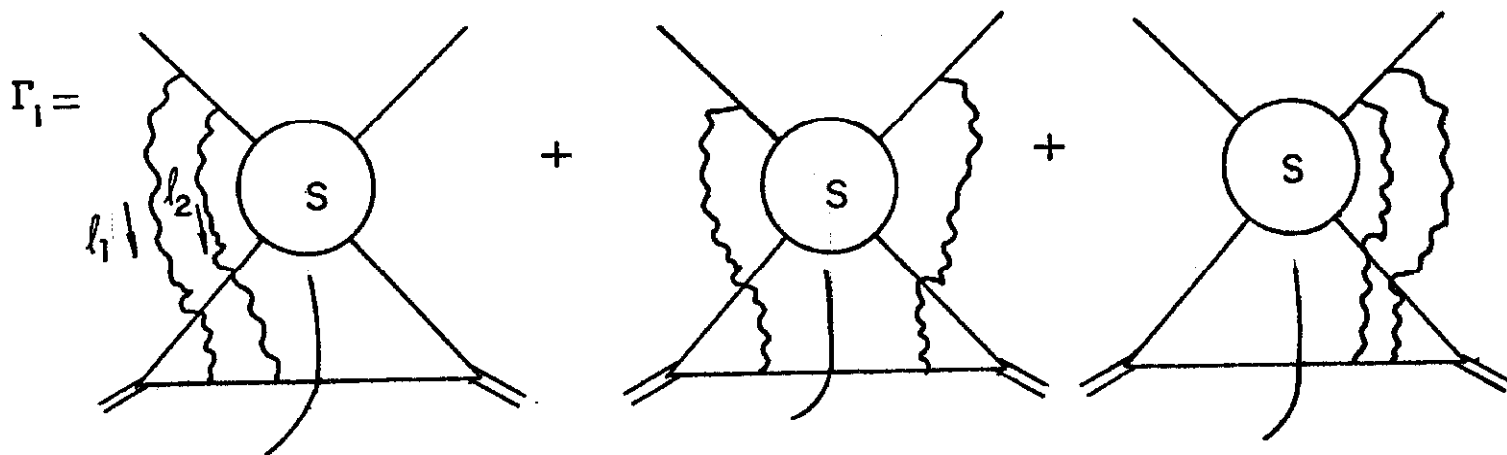


FIG. 3.3

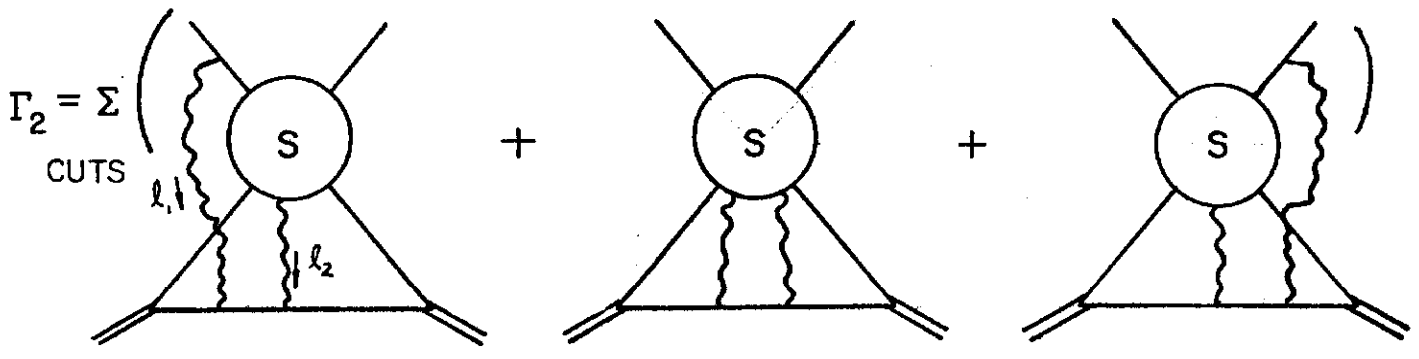


FIG. 3.4

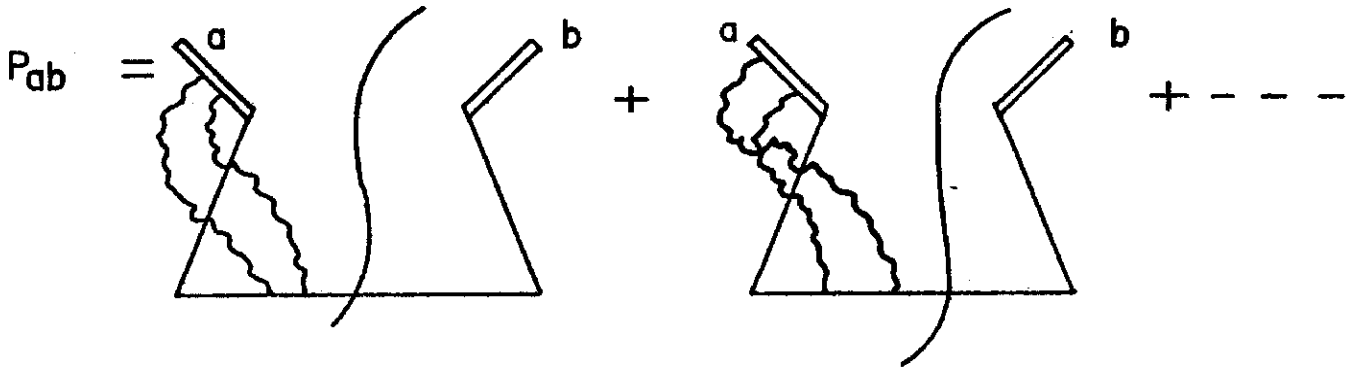


FIG. 3.5

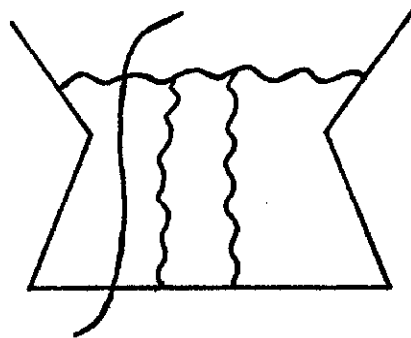


FIG. 3.6

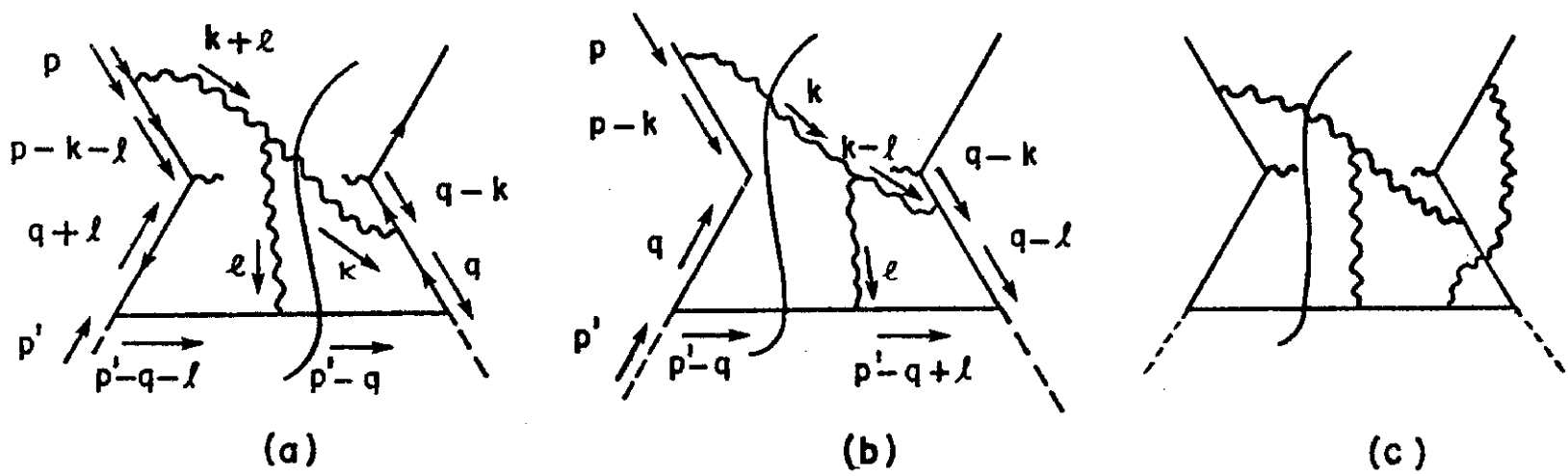


FIG. 4.1

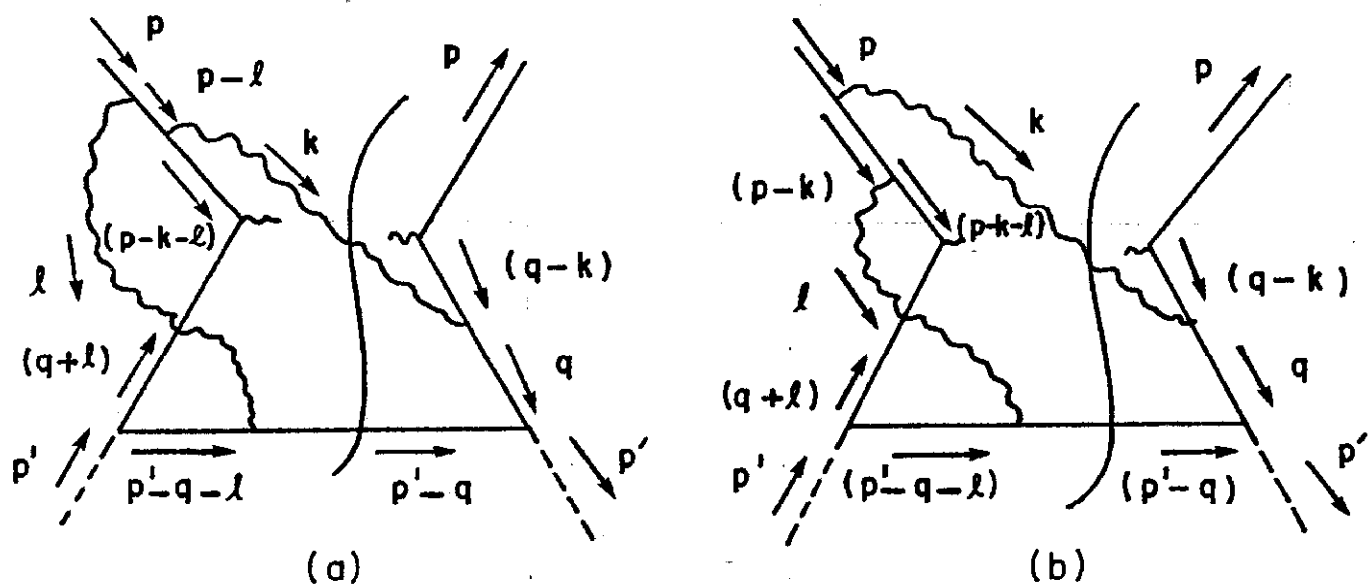
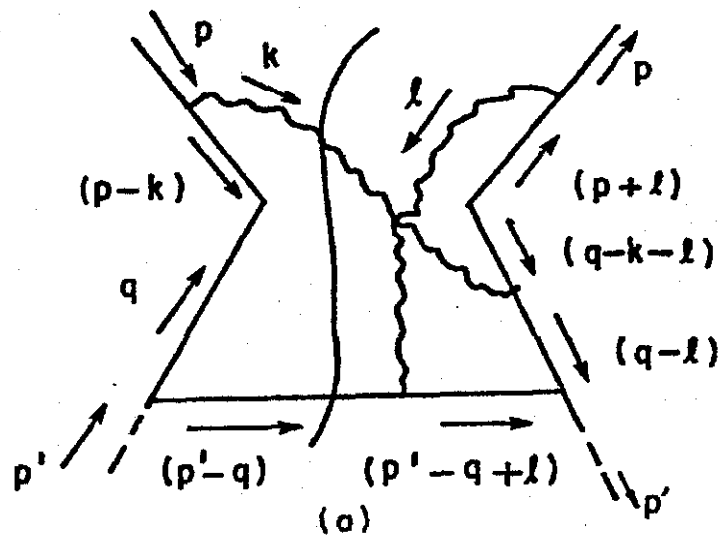
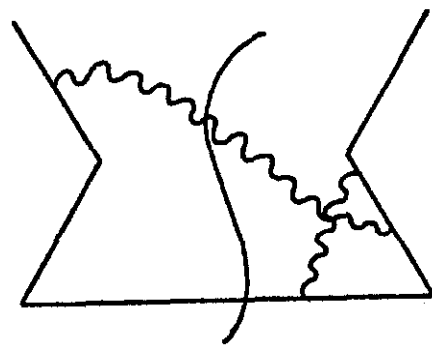


FIG. 4.2



(a)
FIG. 4.3



(b)

FIG. 4.3

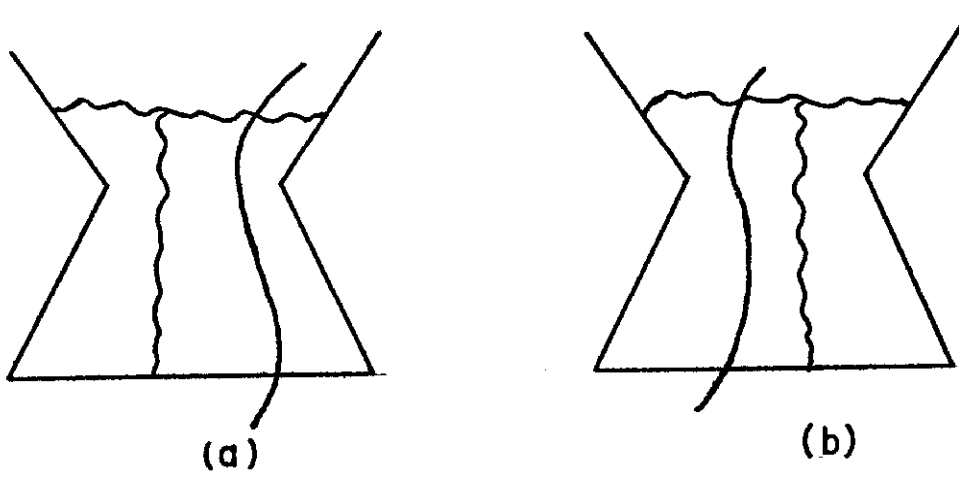
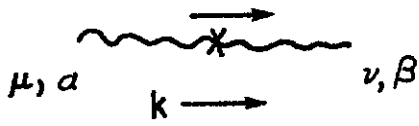
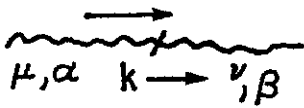


FIG. 4.4



$$-2\pi \delta(k^2) g^{\mu\nu} \delta_{\alpha\beta} \Theta(k_0)$$



$$\frac{-i g^{\mu\nu} \delta_{\alpha\beta}}{(k^0 - |\vec{k}| - i\epsilon)(k^0 + |\vec{k}| - i\epsilon)}$$

FIG. 4.5

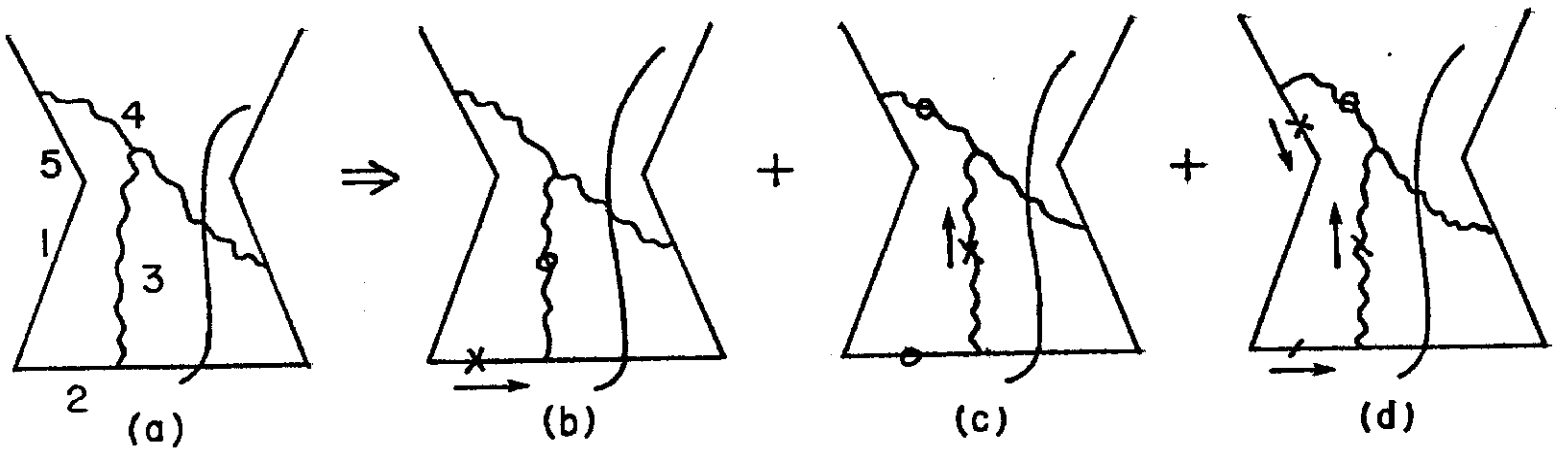


FIG. 4.6

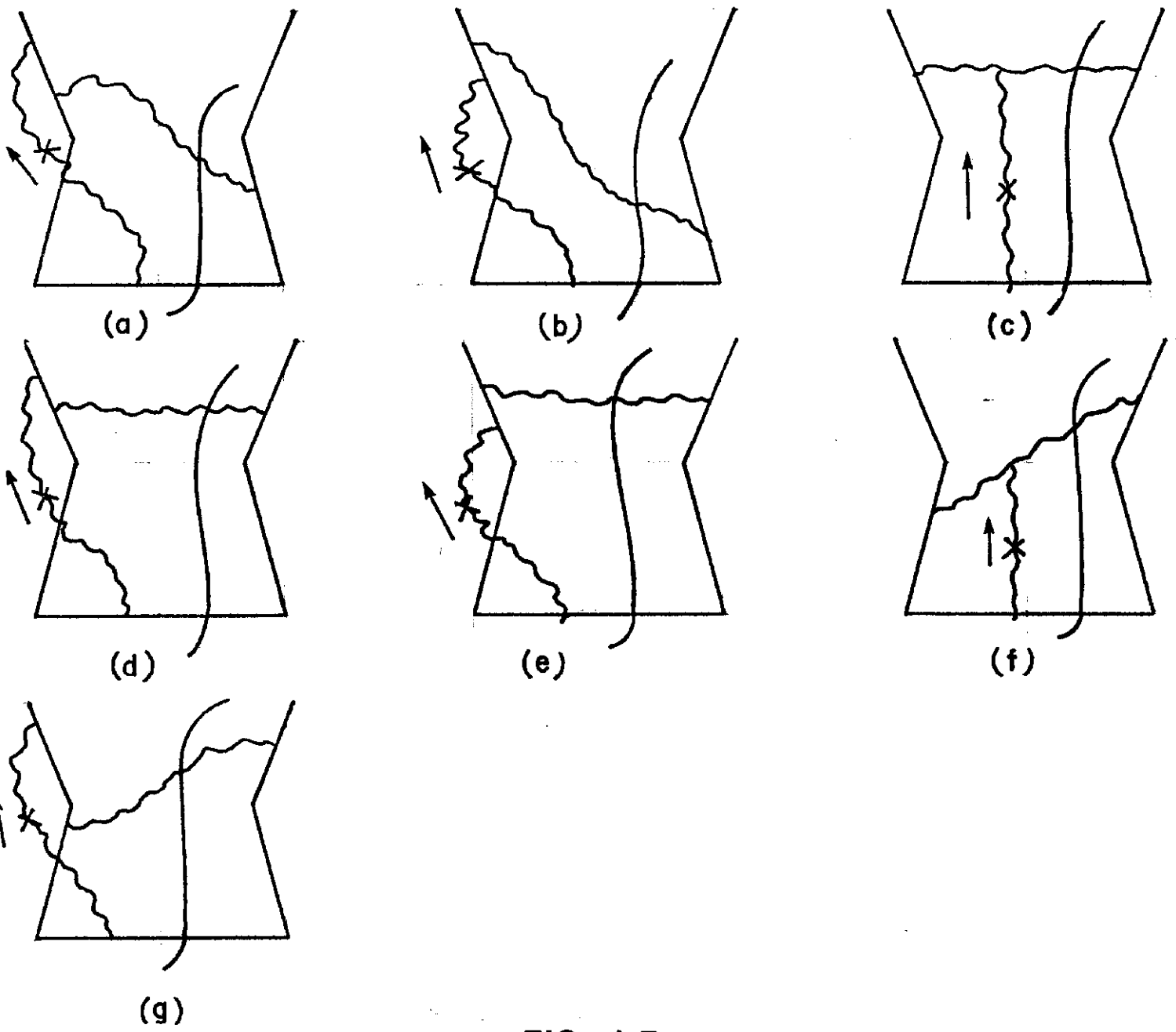


FIG. 4.7

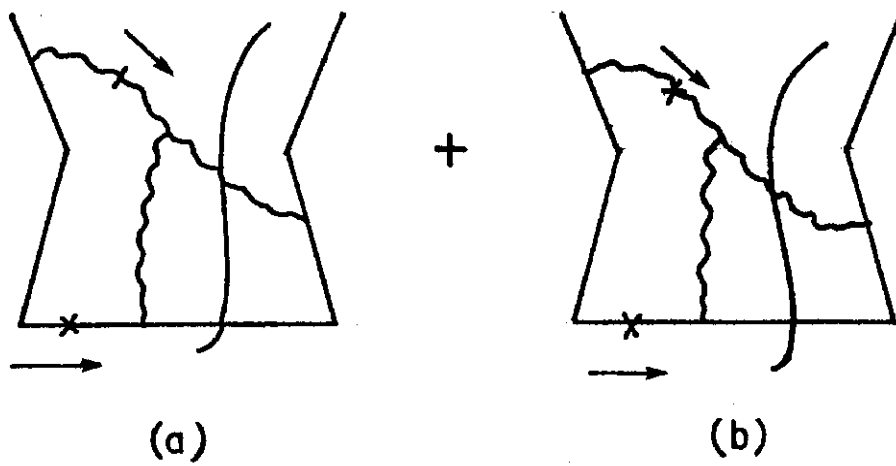


FIG. 4.8

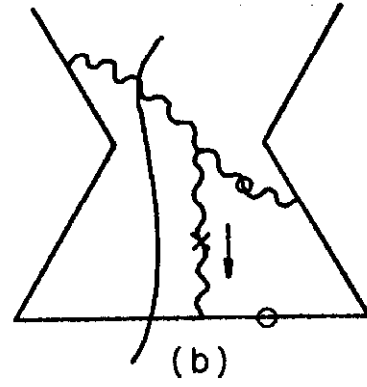
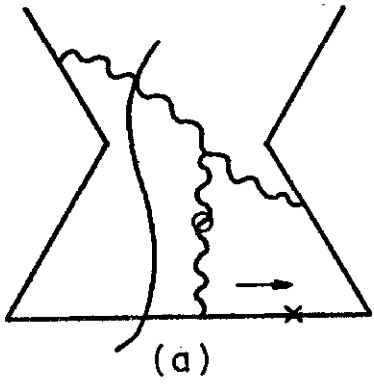


FIG. 4.9

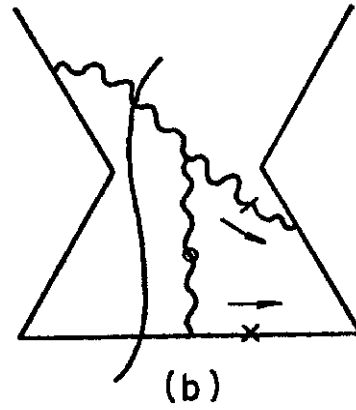
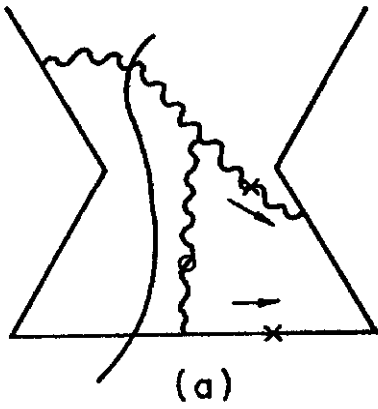


FIG. 4.10

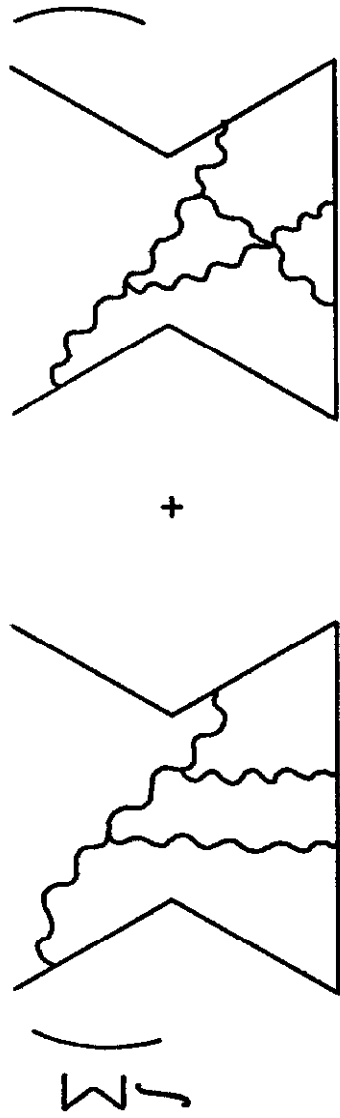


FIG. 5.1

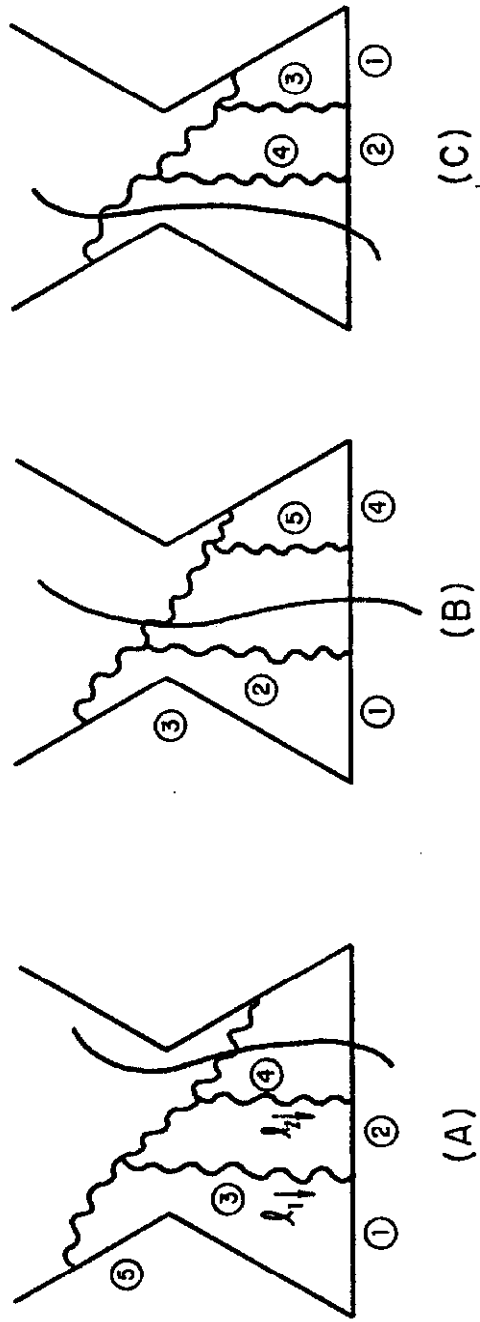


FIG. 5.2

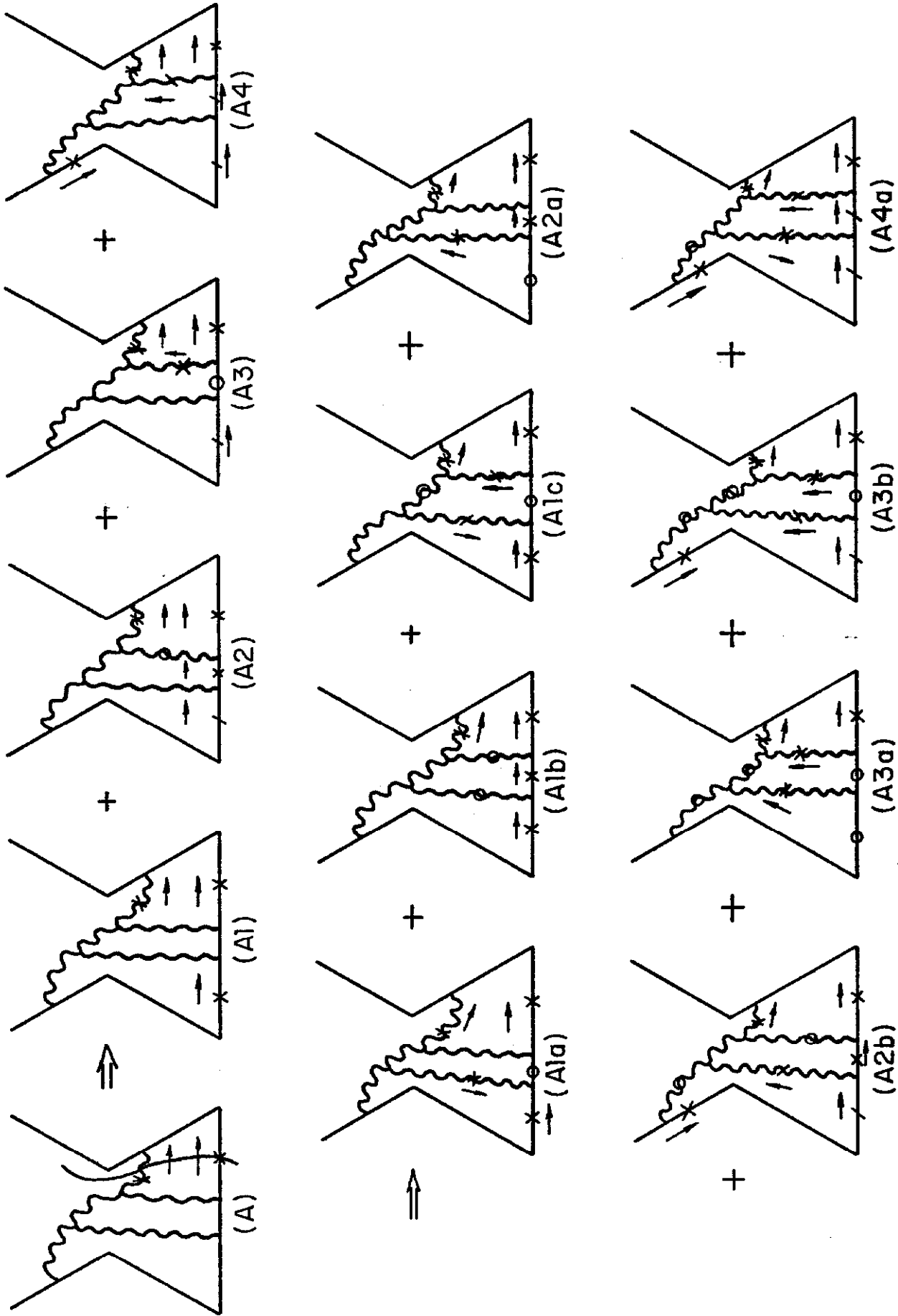


FIG. 5.3

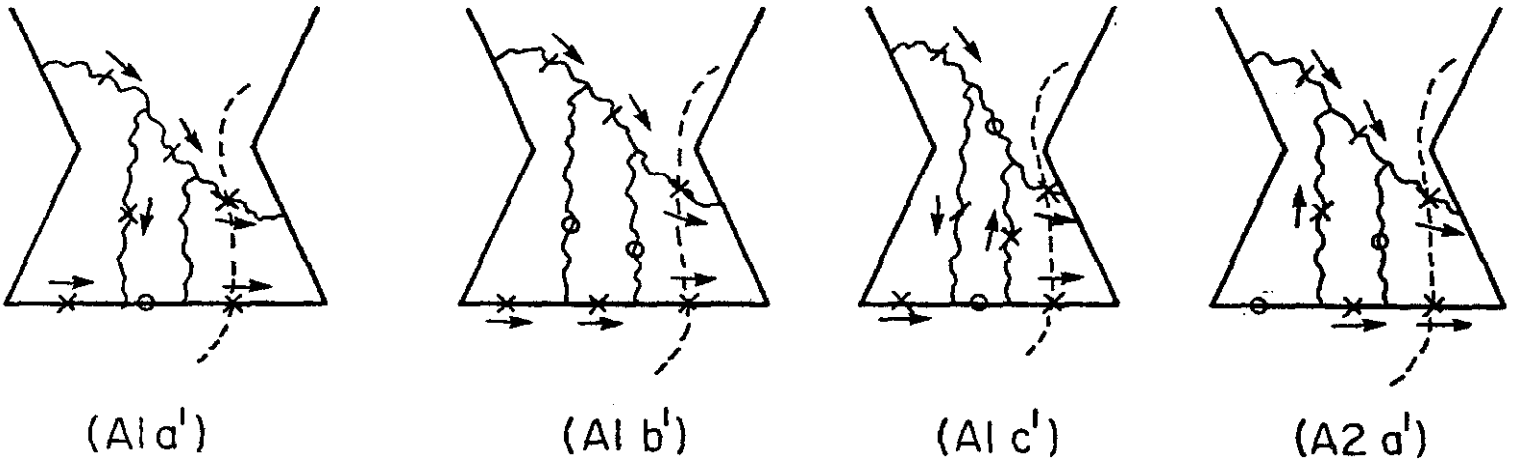


FIG. 5.4

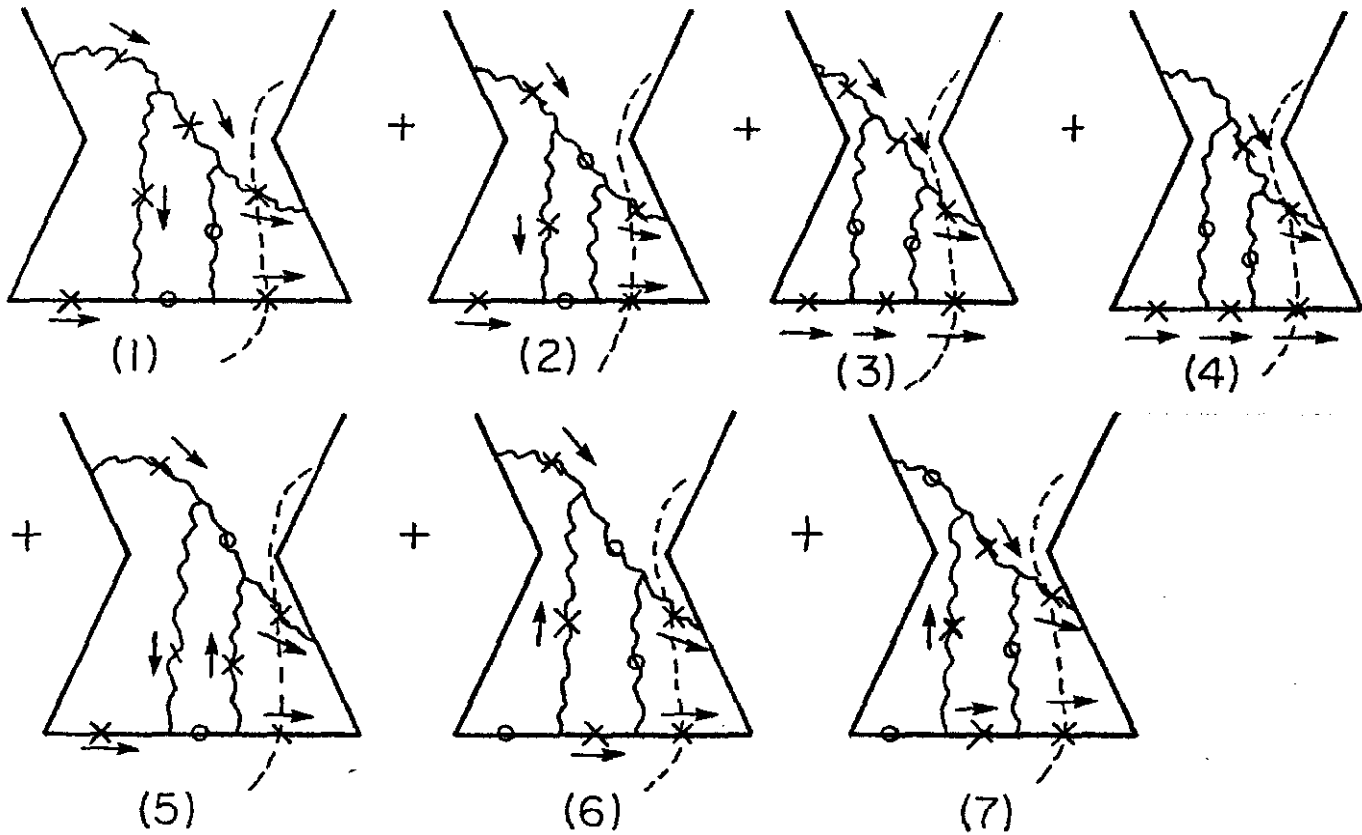


FIG. 5.5

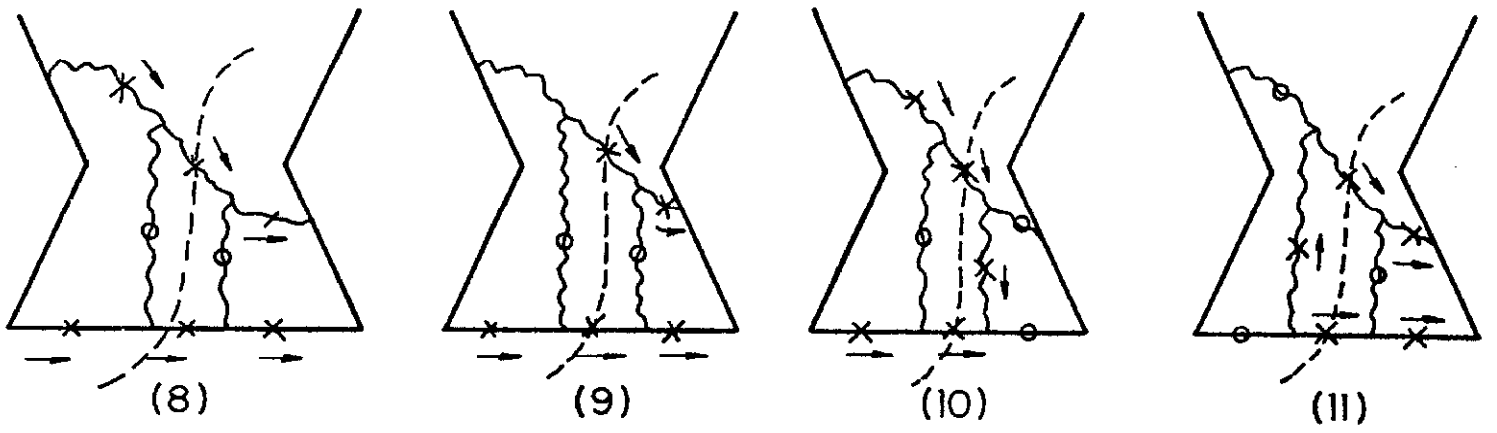


FIG. 5.6

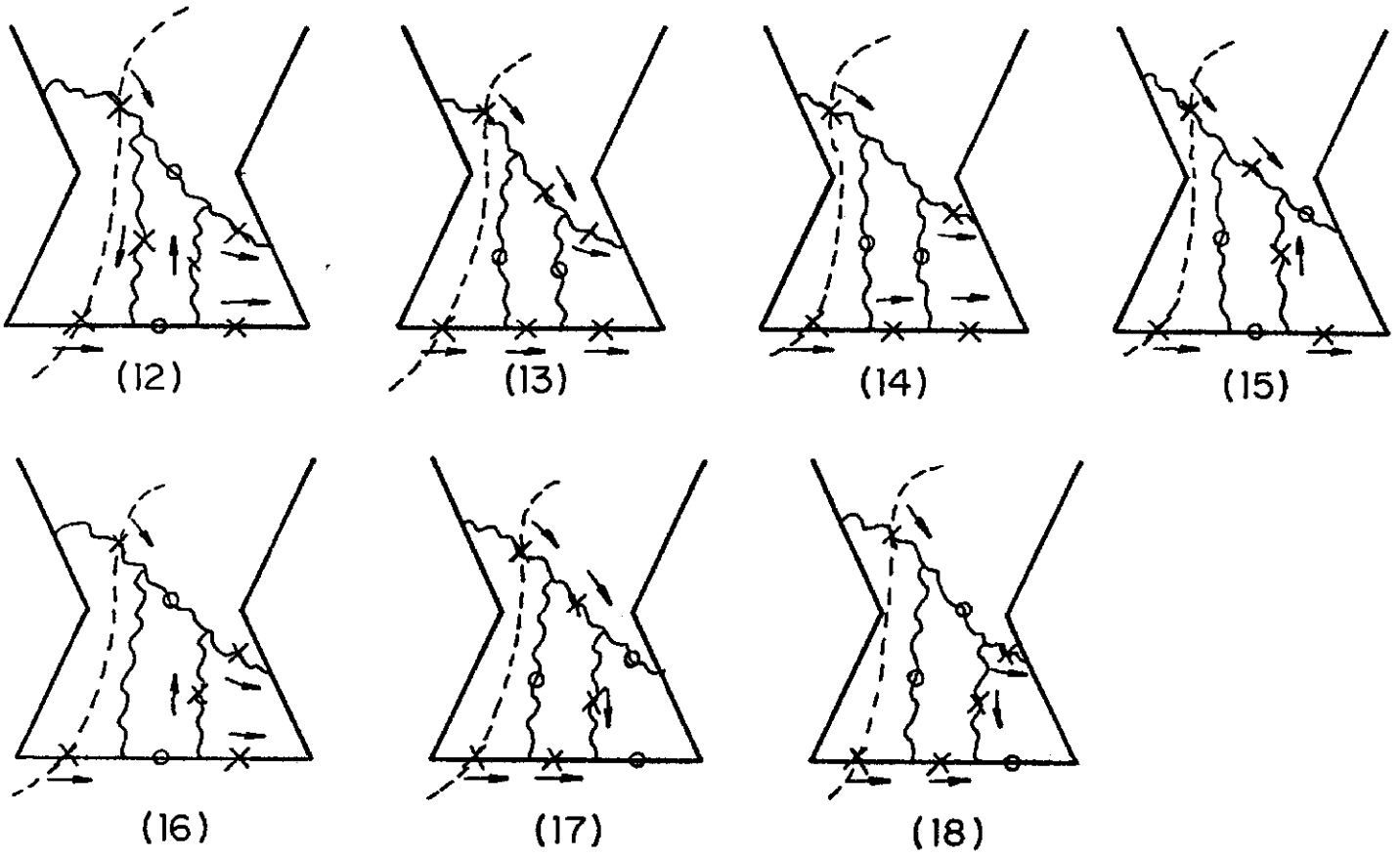


FIG. 5.7

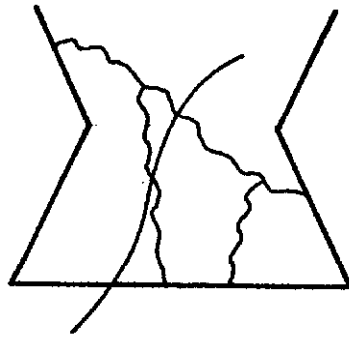


FIG. 5.8

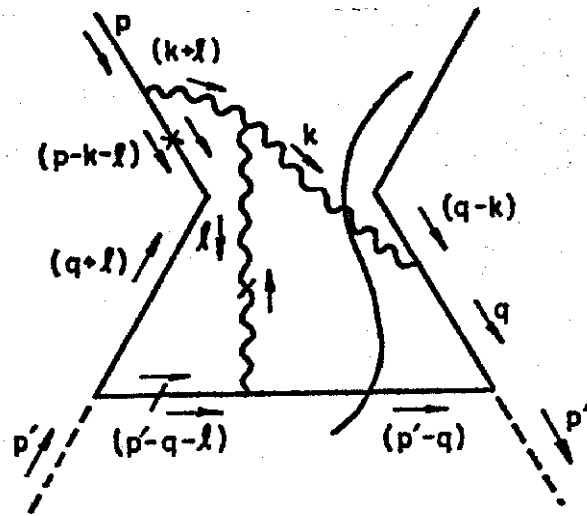


FIG. A.1